

Three-Dimensional Finite-Element Acoustic Analysis of Solid Rocket Motor Cavities

R. M. Hackett*

Vanderbilt University, Nashville, Tenn.

This paper briefly discusses the state-of-the-art of combustion stability analysis of solid propellant rocket motors and the fact that an accurate, unperturbed, acoustical frequency-modal analysis is an initial requirement in the stability analysis. The formulation of a general three-dimensional finite-element structural vibration analysis model is presented in condensed fashion and it is shown how this formulation can be simply modified to yield a fluid vibration analysis model. The resulting model is applied to a simple example problem for the purpose of demonstrating the feasibility of utilizing an existing structural analysis code for a direct three-dimensional acoustic analysis.

Nomenclature

$\{ \}$	= column vector
$[\]$	= row vector
$[\]$	= rectangular or square matrix
$[\]^T$	= transpose of a matrix
$[\]^{-1}$	= inverse of a square matrix
B	= bulk modulus of the fluid
$[D]$	= degree-of-freedom to strain transformation matrix
$[E]$	= material elastic stiffness matrix
$[f]$	= element "equivalent potential energy" matrix
$[F]$	= fluid system "equivalent potential energy" matrix
$[g]$	= element "equivalent kinetic energy" matrix
$[G]$	= fluid system "equivalent kinetic energy" matrix
I	= identity matrix
$[k]$	= element stiffness matrix
$[K]$	= structural system stiffness matrix
$[m]$	= element consistent mass matrix
$[M]$	= structural system consistent mass matrix
N	= shape function
p	= pressure
P	= fluid volume acceleration
Q	= energy functional
R	= fluid mass flow rate
u	= displacement
v	= fluid particle velocity
x, y, z	= coordinate axes
$\{\Delta\}$	= displacement vector
$\{\epsilon\}$	= engineering strain
∇	= gradient
ν	= Poisson's ratio
ω	= natural circular frequency of vibration
ϕ	= velocity potential function
ρ	= mass density
$\{\sigma\}$	= engineering stress

Subscripts

f, g	= energy functional identifiers
i, j, \dots, m	= element node numbers
n	= number of nodal points per element
r, s	= node numbers
S	= structural material
x, y, z	= directions

Superscript

e = element

Introduction

ACOUSTIC oscillations within the combustion chamber of a solid propellant rocket motor create vibratory motions in the unburned propellant and motor case. Present combustion stability technology employs a linear analysis for predicting unsteady motions in the combustion chamber based on the hypothesis that the influences of *combustion* and *flow* may be represented as perturbations of an acoustics problem in a closed chamber. Therefore, before the combustion stability analysis can be carried out, one must have adequate knowledge of the unperturbed normal (harmonic) acoustic modes of oscillation in the cavity, in the absence of combustion and flow.

The cavities in functional rocket motors generally have complex shapes that may include a number of symmetrically placed slots cut into the propellant, the purpose of which is to increase the area of the burning surface. In recent years, the need for experimental acoustic models of such irregular cavity geometries has been reduced through the use of finite-element numerical methods. This technique of analysis was first applied to the prediction of mode structure in the Minuteman II Stage III Motor.¹ The finite-element solutions have been obtained from modified (for the slot effect) two-dimensional axisymmetric models. The NASTRAN computer program² has been generally employed in the analyses conducted to date. This paper attempts to demonstrate the appropriateness and feasibility of a direct three-dimensional finite element acoustic analysis which employs the SAP IV computer code.³

Model Formation

In the finite-element method, a continuum is modeled as an assemblage of elements, connected at discrete locations (nodes). Natural frequencies and mode shapes result from an eigenvalue solution of the equations of motion of the discretely modeled continuum. Applications of the finite-element method in modeling the behavior of a fluid continuum involve several peculiarities not encountered in the usual structural applications.⁴ In the discretization of a fluid continuum, the finite elements represent spatial, rather than material, subregions of the continuum; i.e., instead of representing finite elements of the fluid material, the elements represent subregions in the space through which the fluid moves (Eulerian description of motion). Values of pressure at the nodal points of the element represent the pressures at the nodes rather than of the nodes.

Within each finite element the variation of the pressure p is prescribed by the values of p associated with the nodes

$$p(x, y, z) = [N] \{p\}^e \quad (1)$$

Received Feb. 11, 1976; revision received May 3, 1976. This work was supported by the U.S. Army Missile Command, Redstone Arsenal, Ala. under Basic Agreement DAHCO4-72-A-0001 with Battelle Memorial Institute-Columbus Laboratories.

Index category: Combustion Stability, Ignition, and Detonation.

*Professor of Civil Engineering.

where the vector $[N]$ is composed of suitable *shape functions* of the coordinates and $\{p\}^e$ is the vector of the element nodal point pressures

$$[p]^e = [p_1 p_2 \dots p_m]_n \quad (2)$$

where n is the prescribed number of nodal points per element.

The problem solution is that of determination of the function $p(x, y, z)$ which minimizes the generalized energy functional

$$Q = Q_f + Q_g \quad (3)$$

as formulated for the steady-state waveguide problem in Ref. 5. Considering each individual element

$$\frac{\partial Q^e}{\partial \{p\}^e} = \frac{\partial Q_f^e}{\partial \{p\}^e} + \frac{\partial Q_g^e}{\partial \{p\}^e} \quad (4)$$

With summation over all elements comprising the continuum, the minimization yields

$$\frac{\partial Q}{\partial p} = \sum \frac{\partial Q^e}{\partial \{p\}^e} = 0 \quad (5)$$

and the resulting formulation

$$[F]\{p\} - \omega^2 [G]\{p\} = \{0\} \quad (6)$$

The matrix $[F]$ is obtained by a superpositioning of the individual element matrices $[f]^e$. The matrix $[f]^e$ is symmetric and a typical term is given by

$$f_{rs}^e = \frac{1}{\rho} \left(\int \frac{\partial N_r}{\partial x} \frac{\partial N_s}{\partial x} dx dy dz + \int \frac{\partial N_r}{\partial y} \frac{\partial N_s}{\partial y} dx dy dz + \int \frac{\partial N_r}{\partial z} \frac{\partial N_s}{\partial z} dx dy dz \right) \quad (7)$$

where N_r and N_s are the element shape functions associated with the r th and s th node points, respectively, and ρ is the mass density of the fluid.

The matrix $[G]$ is obtained by superpositioning the element matrices $[g]^e$, given by

$$[g]^e = \frac{1}{B} \int \begin{bmatrix} N_i^2 & N_i N_j & \dots & N_i N_m \\ & N_j^2 & \dots & N_j N_m \\ & & \ddots & \vdots \\ \text{sym} & & & N_m^2 \end{bmatrix} dx dy dz \quad (8)$$

where B is the bulk modulus of the fluid. The solution of Eq. (6) gives the eigenvalues ω^2 and the corresponding mode shapes.

Structural Analogy

When an elastic, deformable, solid continuum is modeled as an assemblage of three-dimensional finite elements, the displacements at any point within each element can be expressed as

$$\{\Delta\} = [N]\{\Delta\}^e = [N_i I N_j I \dots N_m I]\{\Delta\}^e \quad (9)$$

where

$$[\Delta]^e = [u_i] [u_j] \dots [u_m] \quad (10a)$$

$$[u_i] = [u_{xi} u_{yi} u_{zi}], \text{ etc.} \quad (10b)$$

the terms u_{xi} , u_{yi} , and u_{zi} are the displacement components or degrees-of-freedom of the i th node point of the element in the

x , y , and z directions, respectively, and I is the 3×3 identity matrix.

Six strain components are relevant in three-dimensional stress analysis, with the strain matrix, representing the strain condition within an element, defined by

$$\{\epsilon\} = \begin{Bmatrix} \epsilon_{xx} \\ \epsilon_{yy} \\ \epsilon_{zz} \\ \epsilon_{xy} \\ \epsilon_{yz} \\ \epsilon_{zx} \end{Bmatrix} = \begin{Bmatrix} \frac{\partial u_x}{\partial x} \\ \frac{\partial u_y}{\partial y} \\ \frac{\partial u_z}{\partial z} \\ \frac{\partial u_x}{\partial y} + \frac{\partial u_y}{\partial x} \\ \frac{\partial u_y}{\partial z} + \frac{\partial u_z}{\partial y} \\ \frac{\partial u_z}{\partial x} + \frac{\partial u_x}{\partial z} \end{Bmatrix} \quad (11)$$

Considering Eqs. (9)–(11), it can be shown that

$$\{\epsilon\} = [D]\{\Delta\}^e = [D_i D_j \dots D_m]\{\Delta\}^e \quad (12)$$

where

$$[D_i] = \begin{bmatrix} \frac{\partial N_i}{\partial x} & 0 & 0 \\ 0 & \frac{\partial N_i}{\partial y} & 0 \\ 0 & 0 & \frac{\partial N_i}{\partial z} \\ \frac{\partial N_i}{\partial y} & \frac{\partial N_i}{\partial x} & 0 \\ 0 & \frac{\partial N_i}{\partial z} & \frac{\partial N_i}{\partial y} \\ \frac{\partial N_i}{\partial z} & 0 & \frac{\partial N_i}{\partial x} \end{bmatrix} \text{ etc.} \quad (13)$$

The six stress components, defining the stress condition within an element, are given by the expression

$$\{\sigma\} = \begin{Bmatrix} \sigma_{xx} \\ \sigma_{yy} \\ \sigma_{zz} \\ \sigma_{xy} \\ \sigma_{yz} \\ \sigma_{zx} \end{Bmatrix} = [E]\{\epsilon\} \quad (14)$$

The *orthotropic* $[E]$ matrix is simply defined through its inverse:

$$[E]^{-1} = \begin{bmatrix} \frac{1}{E_{xx}} & -\frac{\nu_{xy}}{E_{yy}} & -\frac{\nu_{xz}}{E_{zz}} & 0 & 0 & 0 \\ -\frac{\nu_{yx}}{E_{xx}} & \frac{1}{E_{yy}} & -\frac{\nu_{yz}}{E_{zz}} & 0 & 0 & 0 \\ -\frac{\nu_{zx}}{E_{xx}} & -\frac{\nu_{zy}}{E_{yy}} & \frac{1}{E_{zz}} & 0 & 0 & 0 \\ 0 & 0 & 0 & \frac{1}{E_{xy}} & 0 & 0 \\ 0 & 0 & 0 & 0 & \frac{1}{E_{yz}} & 0 \\ 0 & 0 & 0 & 0 & 0 & \frac{1}{E_{zx}} \end{bmatrix} \quad (15)$$

where the twelve elastic material constants, $E_{xx}, \dots, E_{xy}, \dots, \nu_{xy}, \dots$ are directional with respect to the x, y, z axes.

The structural element stiffness matrix is defined by

$$[k]^e = \int [D]^T [E] [D] dx dy dz \quad (16)$$

The derivation of Eq. (16) is found in numerous reference texts on the finite element method.^{6,7}

The structural element consistent mass matrix for the three-dimensional element is given by

$$[m]^e = \rho_s \int [N]^T [N] dx dy dz \quad (17)$$

where ρ_s is the mass density of the structural material. The derivation of Eq. (17) is also common in numerous reference texts on the finite-element method.^{7,8}

If, in Eq. (15), the values of $\nu_{xy}, \nu_{yz}, \nu_{zx}, \nu_{xz}, \nu_{zy}$, and ν_{yx} are set equal to zero, and the values of $E_{xx}, E_{yy}, E_{zz}, E_{xy}, E_{yz}$, and E_{zx} are set equal to the inverted value of the density of the fluid, ρ^{-1} and if two of the three displacement degrees-of-freedom at each nodal point are restrained, the structural element stiffness matrix of Eq. (16) becomes equivalent to the fluid element matrix defined by Eq. (7). Likewise, if, in Eq. (17), the value of ρ_s is set equal to the inverted value of the bulk modulus of the fluid, B^{-1} , with the same two displacement degrees-of-freedom restrained, the structural element consistent mass matrix becomes equivalent to the fluid element matrix of Eq. (8). The solution of Eq. (6) can then be obtained through the utilization of a standard structural analysis computer program.

To carry the analogy further, with the structural displacement u_x analogous to the pressure p (having suppressed the u_y and u_z displacement components), Eq. (11) can be written as

$$\{\epsilon\} = \begin{Bmatrix} \epsilon_{xx} \\ 0 \\ 0 \\ \epsilon_{xy} \\ 0 \\ \epsilon_{zx} \end{Bmatrix} = \begin{Bmatrix} \frac{\partial u_x}{\partial x} \\ 0 \\ 0 \\ \frac{\partial u_x}{\partial y} \\ 0 \\ \frac{\partial u_x}{\partial z} \end{Bmatrix} \quad (18)$$

or, from Eqs. (12) and (13)

$$\{\epsilon\} = \begin{bmatrix} \frac{\partial N_i}{\partial x} & \frac{\partial N_j}{\partial x} & \dots & \frac{\partial N_m}{\partial x} \\ 0 & 0 & \dots & 0 \\ 0 & 0 & \dots & 0 \\ \frac{\partial N_i}{\partial y} & \frac{\partial N_j}{\partial y} & \dots & \frac{\partial N_m}{\partial y} \\ 0 & 0 & \dots & 0 \\ \frac{\partial N_i}{\partial z} & \frac{\partial N_j}{\partial z} & \dots & \frac{\partial N_m}{\partial z} \end{bmatrix} \begin{Bmatrix} u_{xi} \\ u_{xj} \\ \vdots \\ u_{xm} \end{Bmatrix} \quad (19)$$

Equation (19), then, allows a direct computation of the pressure gradient ∇p , which is analogous to the element strain $\{\epsilon\}$, since

$$\nabla p_x = p_i \frac{\partial N_i}{\partial x} + p_j \frac{\partial N_j}{\partial x} + \dots + p_m \frac{\partial N_m}{\partial x}, \text{ etc.} \quad (20)$$

The gas particle velocity components can then be computed from the equation

$$\{v\} = -(1/\rho\omega) \nabla p \quad (21)$$

where ω is the natural circular frequency obtained from the eigenvalue and

$$[v] = [v_x \ v_y \ v_z] \quad (22)$$

The gas particle velocity is thus shown to be analogous to the structural element stress.

Also, in addition to the normal acoustic modes of a rocket chamber, combustion stability calculations require a knowledge of incompressible potential flow (mean flow). The consideration of fluid incompressibility ($B^{-1}=0$) and the introduction of a "generalized nodal force" vector $\{P\}$ into Eq. (6) will yield the expression

$$[F]\{p\} = \{P\} \quad (23)$$

The velocity potential function φ is related to the pressure by

$$p = \rho(d\varphi/dt) \quad (24)$$

and the mass flow rate R_i into the fluid chamber at any point is related to the volume acceleration through the expression

$$P_i = dR_i/dt \quad (25)$$

Substituting Eqs. (24) and (25) into Eq. (23) results in a matrix equation for the potential field

$$\rho[F]\{\varphi\} = \{R\} \quad (26)$$

with $\{R\}$ being zero at impermeable boundaries. The mean stream velocity components can then be computed from the equation

$$\nabla \varphi_x = \varphi_i \frac{\partial N_i}{\partial x} + \varphi_j \frac{\partial N_j}{\partial x} + \dots + \varphi_m \frac{\partial N_m}{\partial x}, \text{ etc.} \quad (27)$$

the $\varphi_i, \varphi_j, \dots, \varphi_m$ values being obtained from the solution of Eq. (26). Thus, the simple modification of input data to a structural analysis code will yield this information pertinent to a combustion stability analysis.

Example Application

A simple example was selected to demonstrate the utilization of the structural computer code SAP IV for an acoustic analysis. The solid propellant grain/cavity geometry for the problem selected is shown in Fig. 1. The three-

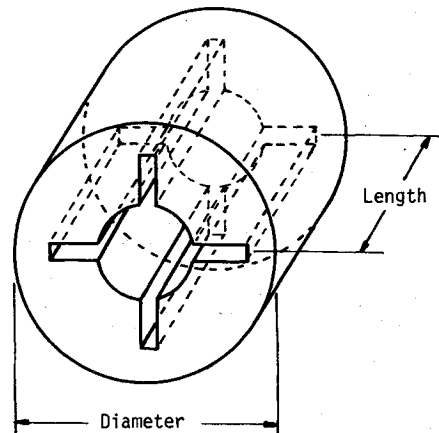


Fig. 1 Solid propellant configuration.

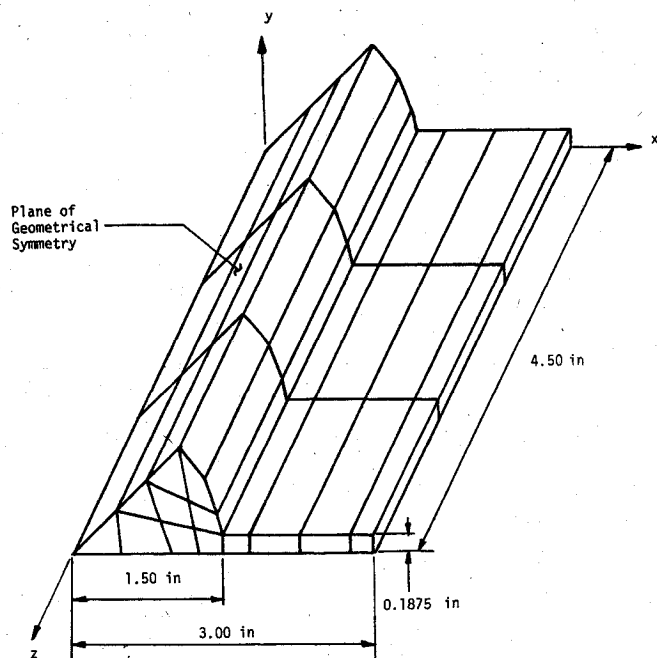


Fig. 2 Three-dimensional finite-element model.

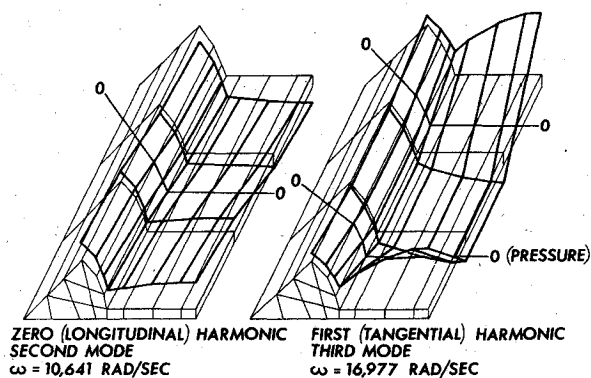


Fig. 3 Example cavity surface acoustic pressure modes (nodal point pressures plotted on vertical scale).

dimensional, finite-element model of a repeating segment of the acoustic cavity is shown in Fig. 2. A coarse mesh was used since the purpose of the example is to demonstrate the ap-

plication and not to obtain quantitative results. For this problem an eight-node brick element having three degrees-of-freedom (two suppressed to yield the fluid element) per node was used.

The properties of the cavity gas used in the analysis were a density of 1.1463×10^{-7} (lb-sec²/in.⁴) and a bulk modulus of 20.59 (lb/in.²). The use of the structural code for this acoustic analysis presumes rigid cavity/propellant boundaries.

The first three modes of the zero (longitudinal) and first and second (tangential) acoustic harmonics were obtained by varying the boundary conditions of the repeating cavity segment modeled in Fig. 2. The modes associated with the zero harmonic were obtained by restraining the nodes located at the intersection of the x and y, the modes associated with the first harmonic were obtained by restraining the nodes located on the y axis, and the modes associated with the second harmonic were obtained by restraining the nodes located on the plane bisecting the slot axes. The nodal point pressures are the predesignated unrestrained directional displacements in the output data. The results of two of the nine cases run are shown plotted in Fig. 3.

Conclusions

It has been demonstrated that three-dimensional finite-element acoustic analyses may be carried out directly through the utilization of existing structural finite-element codes. Slight modifications may be easily made to obtain gas particle velocities from the solution.

References

- ¹Final Report on the Investigation of Pressure Oscillations During Firing of the Minuteman II Stage II Motor," Hercules Inc., Magna, Utah, MTO-1124-34, Jan. 1971.
- ²MacNeal, R.H., "The NASTRAN Theoretical Manual (Level 15)," NASA SP-221 (01), April 1972.
- ³Bathe, K.-J., Wilson, E.L., and Peterson, F.E., "SAP IV", Col. of Eng., University of Calif., Berkeley, Calif., Rept. EERC 73-11, June 1973 (revised April 1974).
- ⁴Oden, J.T. and Somogyi, D., "Finite-Element Applications in Fluid Dynamics, *Proceedings of the ASCE*, Vol. 95, 1969, pp. 821-826.
- ⁵Arlett, P.L., Bahrani, A.K., and Zienkiewicz, O.C., "Application of Finite Elements to the Solution of Helmholtz's Equation," *Proceedings of the IEE*, Vol. 115, Dec. 1968, pp. 1762-1766.
- ⁶Zienkiewicz, O.C., *The Finite Element Method in Engineering Science*, McGraw-Hill, London, 1971.
- ⁷Gallagher, R.H., *Finite Element Analysis—Fundamentals*, Prentice-Hall, Englewood Cliffs, N.J., 1975.
- ⁸Przemieniecki, J.S., *Theory of Matrix Structural Analysis*, McGraw-Hill, New York, 1968.